Journal of Medicinal Chemistry

ARTICLE

pubs.acs.org/jmc

N-(2-{3-[3,5-Bis(trifluoromethyl)phenyl]ureido}ethyl)-glycyrrhetinamide (6b): A Novel Anticancer Glycyrrhetinic Acid Derivative that Targets the Proteasome and Displays Anti-Kinase Activity

Benjamin Lallemand,[†] Fabien Chaix,[§] Marina Bury,[‡] Céline Bruyère,[‡] Jean Ghostin,[§] Jean-Paul Becker,[⊥] Cédric Delporte,[#] Michel Gelbcke,[#] Véronique Mathieu,[‡] Jacques Dubois,[†] Martine Prévost,[⊥] Ivan Jabin,[§] and Robert Kiss*[,‡]

[†]Laboratoire de Chimie Bioanalytique, Toxicologie et Chimie Physique Appliquée, [‡]Laboratoire de Toxicologie, and [#]Laboratoire de Chimie Pharmaceutique Organique, Faculté de Pharmacie, Université Libre de Bruxelles (ULB), and [§]Laboratoire de Chimie Organique and [⊥]Laboratoire de Structure et Fonction des Membranes Biologiques, Faculté des Sciences, ULB, Brussels, Belgium

Supporting Information

ABSTRACT: 18-β-Glycyrrhetinic acid (GA; **1**) and many of its derivatives are cytotoxic in cancer cells. The current study aims to characterize the anticancer effects of 17 novel **1** derivatives. On the basis of these studies, *N*-(2-{3-[3,5-bis(trifluoromethyl)-phenyl]ureido}ethyl)-glycyrrhetinamide (**6b**) appeared to be the most potent compound, with IC_{50} *in vitro* growth inhibitory concentrations in single-digit micromolarity in a panel of 8 cancer cell lines. Compound **6b** is cytostatic and displays similar efficiency in apoptosis-sensitive versus apoptosis-resistant cancer cell lines through, at least partly, the inhibition of the activity of a cluster of a dozen kinases that are implicated in cancer cell proliferation and in the control of the actin cytoskeleton organization. Compound **6b** also inhibits the activity of the 3 proteolytic units of the proteasome. Compound **6b** thus represents an interesting hit from which future compounds could be derived to improve chemotherapeutic regimens that aim to combat cancers associated with poor prognoses.

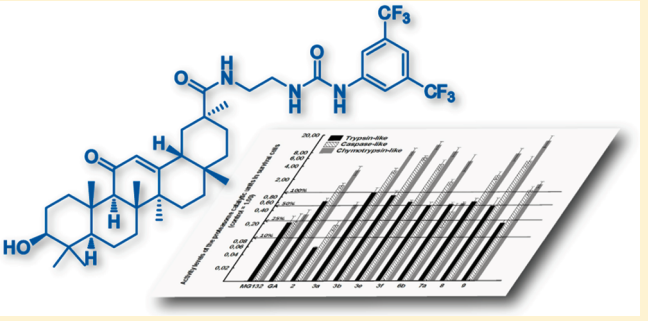

INTRODUCTION

18-β-Glycyrrhetinic acid (GA; **1**) is the main constituent of *Glycyrrhiza glabra*, which has long been used as an antitussive, anti-inflammatory, antiulcer, antiallergic, immunotropic, and hypolipidemic agent.[1] The *in vitro* growth inhibiting activity of **1** was reported three decades ago in mouse[2] and human[3] cancer cell lines, and the **1**-induced *in vivo* activity has also been reported in various experimental cancer models.[4−6] **1** displays both cytostatic[5,7,8] and cytotoxic[7,9] effects in cancer cells, depending on the concentrations, the cell line, and durations of treatment. Cytostatic effects are mediated through the arrest of cancer cells into the G1 phase of the cell cycle as it was shown for **1** and related compounds including ursolic acid and 18β-erythrotriol at 20−25 μM range concentrations.[7]

The **1**-induced cytotoxic effects in cancer cells occur at higher doses and relate to pro-apoptotic stimuli.[4,7,9−11] Indeed, **1** at micromolar concentrations, when added to rat liver mitochondria, induces swelling, loss of membrane potential, pyridine nucleotide oxidation, and release of cytochrome *c* and apoptosis inducing factor.[10] Salvi et al.[10] argue that altogether these data indicate that **1** is an inducer of mitochondrial permeability transition that triggers the pro-apoptotic pathway. Lee et al.[9] report that **1** potentiates the apoptotic effects of trichostatin A, a histone deacetylase inhibitor, in ovarian cancer cells by increasing the activation of the caspase-8-dependent pathway as well as the activation of the mitochondria-mediated cell death.

Schwarz and Csuk[12] have claimed that improving the antitumor activity of **1** without affecting its pro-apoptotic effects is expected to be a major challenge of the derivatization of **1**. However, the aim of the current study was to obtain cytostatic and noncytotoxic (pro-apoptotic) **1** derivatives because many cancers develop acquired chemoresistance during chronic treatment with cytotoxic drugs in the form of the multidrug resistance (MDR) phenotype.[13,14] In addition, various cancer types display intrinsic resistance to pro-apoptotic stimuli, and thus to conventional chemotherapy and radiotherapy. One solution to apoptosis resistance and to the MDR phenotype entails supplementing cytotoxic therapeutic regimens with cytostatic agents.

Received: March 11, 2011
Published: September 02, 2011

We have based our **1**-related derivatization strategy on the fact that **1** and several **1** derivatives are already known to target various kinases[15−19] or to act as proteasome inhibitors.[20] **1** and its derivatives can also target peroxysome proliferator-activated receptors (PPARs),[15,21−24] which control the expression of networks of genes that encode proteins involved in all aspects of lipid metabolism.[25] In addition, PPARs are tumor growth modifiers that act via the regulation of cancer cell apoptosis, proliferation, and differentiation and also through their action on the tumor cell environment, angiogenesis, inflammation, and immune cell functions.[25,26]

The current study characterizes the *in vitro* anticancer activity of 17 novel **1** derivatives and 3 **1** derivatives that have already been described in the literature, namely, compounds **2**,[27] **8**,[28] and **9**[24] (see Figure 1 and Table 1 for the chemical structures). The IC_{50} *in vitro* growth inhibitory concentration of each compound has been determined in 8 cancer cell lines, leading to a structure−activity relationship. The influences of the most interesting compounds have then been analyzed at the levels of proteasome activity inhibition, supported by a molecular docking analysis. The PPAR-γ activation and the inhibition of several kinases have also been evaluated. Lastly, the pro-apoptotic effects of **1** and **6b** have been characterized in two cancer cell lines.

CHEMISTRY

To increase the anticancer activity of **1** and to obtain potent cytostatic compounds, various families of derivatives have been synthesized through chemical modifications at the carboxylic acid group (see R1 in Figure 1 and Table 1).

First, monoamides (**3a**−**f**) were synthesized through peptidic coupling reactions between **1** and various primary amines (Scheme 1). These reactions were conducted in the presence of *N*,*N*′-dicyclohexylcarbodiimide (DCC) and hydroxybenzotriazole (HOB*t*) and produced the desired derivatives in approximately 60−80% yields after flash chromatography (FC) purification (see the Supporting Information). The keto derivative **3e** was prepared by the oxidation of **3d**. In addition to these monoamides, we were also interested in the grafting of a primary amino group to have ready access to different families of compounds. Thus, the peptidic coupling reaction was also applied to the monoprotected ethylenediamine,[29] leading to a 64% yield of the amido derivative **5**. A subsequent deprotection of the amino group under acidic conditions produced the versatile intermediate **2**[27] in 97% yield. Reaction of **2** either with acyl chlorides, isocyanates, or thioisocyanates led to diamido (**4a**−**e**), ureido (**6a**−**c**), and thioureido (**7a**,**b**) derivatives, respectively, in good yields after FC purification.

Finally, the reference compounds, **8**[28] and **9**,[24] were synthesized according to procedures described in the literature (see the Supporting Information).

RESULTS

Determination of the IC_{50} *in Vitro* Growth Inhibitory Concentration. The IC_{50} *in vitro* growth inhibitory concentrations of all of the synthesized compounds were determined with a MTT colorimetric assay[30−33] in a panel of seven human and one mouse cancer cell lines after three days of culturing the cancer cells with the respective drugs (Table 1).

The histological origin of each cancer cell line in this study is detailed in the legend of Table 1, and of these eight cancer cell lines, the human U373[33,34] and T98G[34] GBM, the A549 NSCLC,[35,36] and the SKMEL-28[37] cell lines were previously demonstrated to show various levels of resistance to distinct pro-apoptotic stimuli. Similarly, the sensitivity to apoptosis was reported for the human Hs683 oligodendroglioma,[33,34] the MCF-7 breast,[38] the PC-3 prostate[38] cell lines, and for the mouse B16F10[37] melanoma cell line. Table 1 shows that all compounds under study display similar growth inhibitory activity whether the cancer cell lines are sensitive or rather resistant to pro-apoptotic stimuli. It must nevertheless be emphasized that most **1**-related monoamides, i.e., **3a**, **3b**, **3d**, **3e**, and **3f**, seem to be less efficient in apoptosis-resistant (U373, T98G, A549, SKMEL-28) than in apoptosis-sensitive cell lines (Hs683, MCF-7, PC-3, B16F10) (Table 1). However, these differences did not reach statistical levels of significance, because $n = 4$ in each group only, and because heterogeneous responses were observed between the cancer cell lines with respect to a given compound (Table 1).

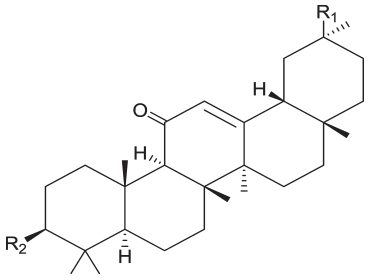

Figure 1. Chemical structure of GA (**1**) illustrating the R1 and R2 sites on which modifications were carried out (see Table 1).

Compound 1 is Cytotoxic, while Compound 6b Is Cytostatic. Flow cytometry analyses revealed that **1** at its IC_{50} *in vitro* growth inhibitory concentrations (see Table 1) induced slight pro-apoptotic effects in U373 GBM cells, but marked ones in A549 ones (Figure 2A) as expected from data published in the literature.[7,9] **1** did not induce cytostatic effects in U373 GBM and A549 NSCLC cells as revealed by the absence of accumulation of cancer cells in the G1 phase of the cell cycle (Figure 2B), a feature expected to occur when **1** displays cytostatic effects.[7] Compound **6b** appeared cytostatic according to the fact that it did not induce apoptosis in U373 GBM and A549 NSCLC cells (Figure 2A). However, this cytostatic effects did not relate to the accumulation of cancer cells in the G1 phase (Figure 2B), a feature that prompted us to analyze **6b**-induced effects on the kinome and on the proteasome as detailed below.

Characterizing 6b-Induced Effects on a Panel of 333 Kinases. Compound **6b** was assayed at 1 μM in a panel of 333 kinases (see the Supporting Information). **6b** displayed *in vitro* growth inhibitory concentrations that range between 4 and 12 μM among the 8 cancer cell lines analyzed in the current study (Table 1). Therefore, 1 μM represents between 8% and 25% of these *in vitro* growth inhibitory concentrations. In this very low concentration range, **6b** inhibited the activity of the 12 kinases listed in Table 2 by $\geq$50%. Among these kinases, 4 already are inhibitors that have been studied in clinical trials, whereas no inhibitors are being examined in clinical trials for the remaining 8 kinases.

Most, if not all, of these kinases (Table 2), including ALK,[39] BMX,[40] EPHB1 and EPHB4,[41,42] Fes and Fyn,[43,44] FGF-R2,[45] IGFR1,[46] RET,[47] ZAP70,[48] and PAK2,[49] play somewhat important roles in cancer cell proliferation, adhesion, motility and invasion, and thus in cancer cell migration and cancer metastatic processes.

Table 1. Characterization of the *in Vitro* Growth Inhibitory Activity of 17 Novel and 3 (2, 8, 9) Already Known GA (1) Derivatives versus 1 in a Panel of 8 Cancer Cell Lines

Compounds			P[a]	S[b]	IC_{50} *in vitro* growth inhibitory concentrations (μM)[c]							
#	R1	R2	(%)		A549	SKMEL	T98G	HS683	U373	PC3	MCF7	B16F10
1		OH	98	98	>100[d]	92	85	84	83	80	76	37
2	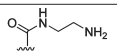	OH	96	90	31	>100	>100	58	32	31	59	30
3a	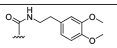	OH	96	86	52	>100	91	59	43	34	34	37
3b	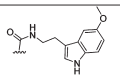	OH	97	94	40	>100	>100	57	75	43	38	31
3c	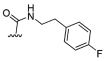	OH	95	95	33	82	46	56	42	33	31	32
3d	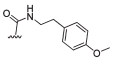	OH	95	91	37	>100	68	61	49	34	36	31
3e	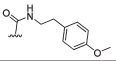	=O	98	93	>100	>100	>100	91	69	52	56	49
3f	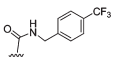	OH	96	95	37	65	67	49	44	35	29	39
4a	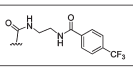	OH	95	95	47	49	62	38	55	53	28	36
4b	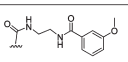	OH	95	99	63	42	77	58	75	72	46	31
4c	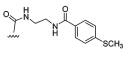	OH	96	99	37	38	54	36	37	47	30	31
4d	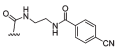	OH	98	92	68	35	77	67	76	72	27	31
4e	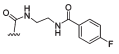	OH	98	98	28	37	35	31	29	30	25	28
5	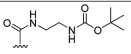	OH	96	93	43	60	73	63	57	41	37	48
6a	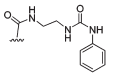	OH	99	96	29	49	30	28	30	32	28	31
6b	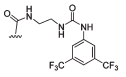	OH	99	98	7	9	12	6	6	8	4	4
6c	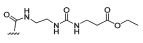	OH	98	99	29	65	71	42	42	46	42	41
7a	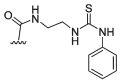	OH	97	94	31	38	25	8	29	9	30	34
7b	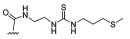	OH	97	93	38	33	35	36	35	39	30	33
8	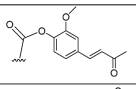	OH	99	68	2	3	3	3	2	2	3	3
9	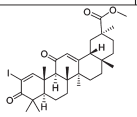		97	89	42	32	6	48	42	36	28	23

[a] P indicates purity. [b] The stability of the products was measured with HPLC analysis following incubation in MEM cell culture medium at 37 °C over 7 days. Results are expressed as the % of the incubated compound recovered. [c] The IC_{50} *in vitro* growth inhibitory concentrations were determined using the MTT colorimetric assay. The cell lines include the following: human U373 (ECACC code 89081403), T98G (ATCC code CRL1690), and Hs683 (ATCC code HTB-138) glioblastoma, the A549 (DSMZ code ACC107) NSCLC, the MCF-7 (DSMZ code ACC115) breast cancer, and the PC-3 (DSMZ code ACC465) prostate cancer and SKMEL-28 (ATCC code HTB-72) melanoma. One mouse cell line, i.e., the B16F10 melanoma model (ATCC code CRL-6475) was also analyzed. [d] Six data points were available for each concentration tested and nine concentrations (from 0.01 to 100 μM, with semilog increases) were available for each cell line.

dx.doi.org/10.1021/jm200285z |*J. Med. Chem.* 2011, 54, 6501–6513

Scheme 1[a]

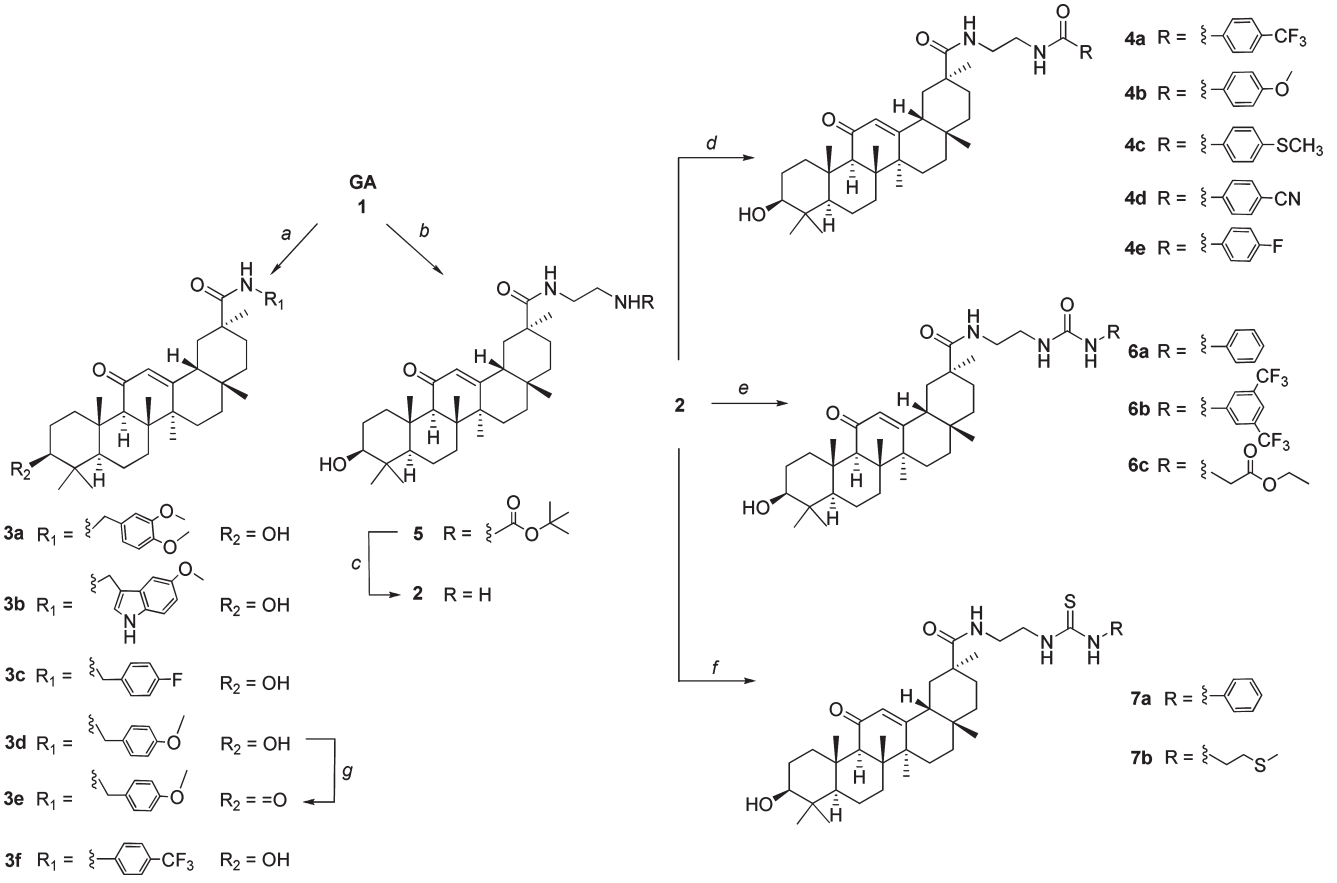

[a] Reagents and conditions: (a) 1°. DCC, HOBt, DIPEA, DMF, RT, 30 min; 2°. R_1NH_2, RT, overnight; (b) 1°. DCC, HOBt, DIPEA, DMF, RT, 30 min; 2°. $H_2N(CH_2)_2NHBoc$, RT, overnight, 64%; (c) TFA, DCM, 0 °C, 3 h, 97%; (d) DMAP, RCOCl, DCM; (e) THF, RNCO, RT, 20 h; (f) THF, RNCS, RT, 20 h; (g) Jones reagent, acetone, 0 °C, 45 min, 98%.

Several Compounds under Study Target the Proteasome. On the basis of the fact that **1** derivatives can target the proteasome, we biochemically analyzed the effects of six **1** derivatives in addition to compounds **1**, **2**, **8**, and **9** on the three proteasome catalytic units, including the trypsin-like, the caspase-like, and the chymotrypsin-like units. Each compound was tested at its mean MTT colorimetric assay-related IC_{50} concentrations calculated on the eight cancer cell lines (see Table 1). The proteasome inhibitor MG-132[50] was analyzed at a concentration of 0.5 μM.

Figure 3A shows that 60 μM **2** inhibited the three proteasome catalytic units with an efficiency that was similar to that of the 0.5 μM MG-132. Compound **6b** (7 μM) also inhibited the three catalytic units of the proteasome, but at a much lower concentration than **2** (Figure 3A). While the remaining compounds, **1** (90 μM), **3a** (60 μM), **3b** (70 μM), **3e** (80 μM), **3f** (50 μM), **7a** (25 μM), **8** (3 μM), and **9** (30 μM), inhibited the activity of the trypsin-like catalytic unit, they also activated the caspase-like and the chymotrypsin-like catalytic units (Figure 3A).

In order to get a deeper insight into the molecular basis of the proteasome recognition by the different compounds, we performed molecular docking experiments at each of the caspase-like (C-L; Figure 3B), trypsin-like (T-L; Figure 3B), or chymotrypsin-like (CT-L; Figure 3B) sites of proteolytic functions. Figure 3B illustrates these three doublets of proteolytic sites in a crystal structure complexed to fellutamide B[51] (PDB code 3D29). The structure of the proteasome has also been determined with bortezomib, the sole antiproteasome marketed compound to date, bound at all six sites. We did not use bortezomib for our docking analyses because it contains a boron atom that is not supported in the default force field used and optimized for the *Glide* software that was employed in this study.

To assess the reliability of our docking procedure, the crystallographic ligand, fellutamide B, was docked in the three different pairs of binding sites of the yeast proteasome after removal of all water molecules and ligands. The docked poses were compared with the positions of the crystal ligand by computing the root-mean-square deviation (rmsd), which measures the distance between the poses. A rmsd value for the backbone atoms was found to range between 0.6 and 2.0 Å for all sites, indicating a high similarity between the docked and the experimental positions of the crystallographic ligand.

Compound **6b**, the molecule exhibiting the best affinity, was docked in the three different catalytic sites. A detailed analysis identified in all three sites two types of binding modes. In one of these two modes, the 3,5-bis(trifluoromethyl)phenyl moiety accommodates the S1 specificity pocket[52] and the diamide group forms several hydrogen bonds. This mode appears to present similarities to the mode of binding of several known peptide inhibitors,[53] which mimic the proteasome susbstrate backbone.

dx.doi.org/10.1021/jm200285z |*J. Med. Chem.* 2011, 54, 6501–6513

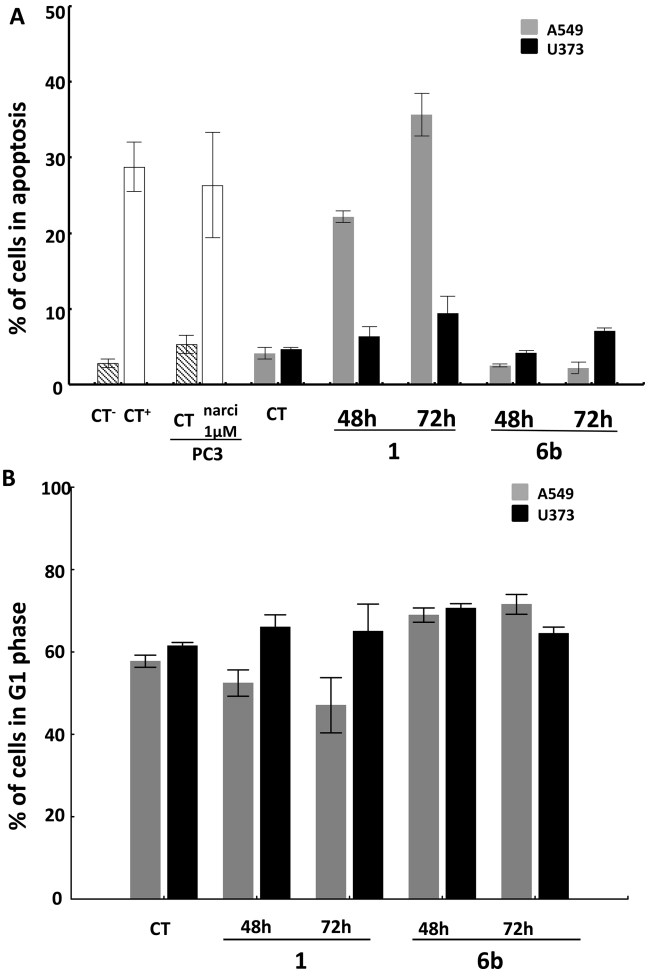

Figure 2. (A) Determination of the percentages of A549 NSCLC and U373 GBM cells undergoing apoptosis during 48 and 72 h of treatment with 80 (U373 cells) and 100 (A549 cells) μM for compound **1** and 10 μM (for both cell lines) for compound **6b**. Negative (Ct^-) and positive (Ct^+) controls available in the kit were used along with 1 μM narciclasine-treated human PC-3 prostate cancer cells as controls for this experiment. (B) Growth rate determination (i.e., the determination of the % of cells in the G1 phase of the cell cycle) for the U373 GBM and A549 NSCLC cells treated as in (C). Each experimental condition was performed in triplicate, and the data are presented as the mean ± SD values.

The second mode which is more largely represented in the chymotrypsin and caspase-like sites depicts the 3,5-bis(trifluoromethyl)phenyl moiety bound in the S3 specificity pocket. This mode agrees with the inhibition potency, at the chymotrypsin-like site and to a lesser extent at the caspase-like site, of proteasome inhibitors containing 3,5-bis(trifluoromethyl)-phenyl at the S3 position.[54] To attempt to discriminate between these two binding modes, we performed docking of **6b** in a series of proteasome crystal structures in complex with different inhibitors, most of them bound to the chymotrypsin-like site (PDB codes 3NZJ, 3MG8, 3MG4, and 3GPJ). Overall, the most common docked pose portrayed the 3,5-bis(trifluoromethyl)phenyl moiety of **6b** in the S3 specificity pocket. Docking experiments including protein flexibility (induced-fit protocol from Schrodinger Inc.) in the form of flexible side chain residues selected in the vicinity of the S1 specificity pocket corroborate this binding mode.

A unique feature of **6b** is to inhibit with a similar potency the three catalytic units, whereas our other GA derivatives exhibit a large discrepancy in their activity toward the different sites. We thus carried out the docking of **3e** in the chymotrypsin-like and the trypsin-like binding sites which feature the largest potency difference. In the chymotrypsin-like site, **3e** occupies none of the specificity pockets in contrast to **6b** (see Figure 3C and D). In the trypsin-like site, however, the best binding poses of **3e** show that its aromatic moiety visits the S1 specificity pocket, as for compound **6b**. Interestingly, a significantly higher potency was measured at the chymotrypsine-like site for a noncovalent inhibitor featuring a 3,4,5-trimethoxybenzylamine at the S3 position relative to the derivative containing only one methoxy.[55]

Several Compounds in this Study Were Found to Inhibit PPAR-γ. On the basis of the fact that **1** derivatives can target PPAR-γ, we also biochemically analyzed PPAR-γ inhibition versus the activation induced by the 10 compounds described above for the proteasome inhibition analyses. The compounds were studied at the same concentrations as those reported above for the proteasome inhibition analyses. Figure 4 shows that **1**, **2**, and **6b** did not significantly ($p > 0.05$; Kruskal–Wallis with Dunn's procedure) modify PPAR-γ activity as compared to the control, whereas the remaining seven **1** derivatives inhibited PPAR-γ activity ($p > 0.05$; Kruskal–Wallis with Dunn's procedure, except for **3f** $p < 0.05$) (Figure 4B).

DISCUSSION

Cancer remains a devastating disease, and the number of cancer-related deaths is still increasing. More than 90% of cancer patients die from tumor metastases, which are intrinsically resistant to apoptosis;[56] therefore, these tumors are unresponsive to a large majority of currently available anticancer drugs, which generally work through apoptosis induction.[57,58] Before metastasizing, many cancer types also display intrinsic resistance to proapoptotic stimuli; these include head and neck cancers,[59] non-small-cell lung cancer (NSCLC),[35,60] melanoma,[61] pancreatic cancer,[62] esophageal cancer,[63,64] and gliomas.[65] As emphasized by Landis-Piwowar et al.,[66] drug resistance limits the effectiveness of treatment options and is a major challenge faced by current cancer research. As detailed below, an additive effect has been observed in cancer cells treated with bortezomib in combination with traditional chemotherapeutics, and in some cases, drug resistance has been overcome.[66] In the same manner, one of the kinases targeted by **6b**, i.e., BMX,[67] is implicated in cancer drug resistance. Thus, **6b**, apart its intrinsic anticancer activity that makes it able to overcome resistance to pro-apoptotic stimuli, could also overcome cancer drug resistance if administered with conventional chemotherapeutics.

The IC_{50} *in vitro* growth inhibitory concentrations of all newly synthesized compounds are lower than that of **1** (Table 1), clearly showing the importance of the amido subunit to increase anticancer activity, at least *in vitro*. According to the fact that the oxidation of the hydroxy group on the C-3 position decreases the *in vitro* anticancer activity (**3d** vs **3e**), this position was not further modified in the frame of the current study. The results reveal that most **1**-related monoamides could display weaker growth inhibitory activity in apoptosis-resistant cancer cell lines (i.e., >100 μM) compared to apoptosis-sensitive cancer cell lines (Table 1). Therefore, monoamide **1** derivatives (**3a**–**f**) do not seem to be appropriate drugs to combat those cancer types associated with poor prognoses because they are able to resist

dx.doi.org/10.1021/jm200285z |J. Med. Chem. 2011, 54, 6501–6513

Table 2. Identification of the Kinases Targeted by Compound 6b at a Concentration of 1 μM[a]

kinases	name or family	% of **6b**-induced inhibition at 1 μM	major cancer types in which the kinase displays significant roles in cell biology	compounds currently in clinical trials targeting this kinase versus cancer types
ALK	Anaplastic lymphoma kinases	69	Anaplastic large cell lymphoma, inflammatory myofibroblastic tumors, nonsmall cell lung cancer, and neuroblastoma	Crizotinib, an oral ALK inhibitor, was demonstrated to provide dramatic clinical benefit with little toxicity in patients with advanced NSCLC
BMX	B-tyrosine kinases family	52	Androgen-independent prostate cancers. Also implicated in the chemoresistance of small-cell-lung cancers, play a role in cell growth and differentiation	None
PAK2	p-21 associated kinases family	51	Ovarian cancers, regule the actin cytoskeleton during cell motility and invasion	None
EPHB1	Eph receptor tyrosine kinases	64	Ovarian cancers; colon cancers, play a role in the cell adhesion and migration	None
EPHB4	Eph receptor tyrosine kinases	64	Ovarian cancers; colon cancers; gastric cancers; prostate cancers, module integrin-mediated adhesion	None
RET	R tyrosine kinases family	48	Thyroid cancers; Multiple endocrine neoplasia type 2 (MEN 2), play a role in the cell adhesion and migration	None
ZAP70	Zeta-chain (TCR) associated protein kinases	67	Chronic lymphocytic leukemia (CLL), play a role in cell migration	None
FGF-R2	Fibroblast growth factor receptor type 2	67	Breast cancers; gastric cancers; endometrial cancers; prostate cancers, play a role in the cell proliferation	AZD2171 - Ki23057 - PD173074 - SU5402
FES	Fes tyrosine kinases	59	Not yet clearly defined	None
FYN	Src kinase family	72	Prostate cancers, play a role in the cell proliferation, morphogenesis and motility	Dasatinib, an orally available small-molecule multikinase inhibitor
IGF-R1	Insulin-like growth factor type 1	64	Breast cancers; colon cancers; head and neck cancers	Dalotuzumab
MATK	Megakaryocyte-associated tyrosine kinases	50	Not yet clearly defined	None

[a] The panel of 333 kinases that have been investigated are provided in the Supporting Information.

pro-apoptotic stimuli. In comparison with monoamido (**3**) and diamido (**4**) groups, the ureido (**6**) and thioureido (**7**) ones lead to a better *in vitro* anticancer activity. Finally, the addition of electron-withdrawing groups on the aromatic part of the ureido moieties (**6a** vs **6b**) seems to reinforce this *in vitro* anticancer activity as revealed by the MTT colorimetric assay.

As discussed below, **6b** emerges as a hit from the current **1** derivatives. At first glance, one could estimate that **6b** would be difficult to be further developed due to its high molecular weight and poor hydrosolubility. However, preliminary data we obtained already indicate that **6b** can be formulated as specific microemulsions for oral and i.v. administrations, a project that is currently ongoing in our laboratory.

Together, these data led us to focus less on the monoamide (**3a**−**f**) and diamido-**1** (**4a**−**e**) derivatives and more on the remaining compounds in this study. We thus decided to pay particular attention to **6b**, which appeared to be the most potent compound from the current series in terms of *in vitro* growth inhibitory activity in a panel of four apoptosis-resistant and four apoptosis-sensitive cancer cells lines (Table 1). In addition, **6b** also appeared to be an actual cytostatic compound as revealed by flow cytometry analyses (Figure 2).

We then analyzed **6b**'s ability to inhibit proteasome activity because **1** and certain of its derivatives have already been shown to act as proteasome inhibitors.[20] Proteasomes are large, multicatalytic proteinase complexes located in the cytosol and in the nucleus of eukaryotic cells.[68,69] The ubiquitin−proteasome system is responsible for the degradation of most intracellular proteins and therefore plays an essential regulatory role in critical cellular processes, including cell cycle progression, proliferation, differentiation, angiogenesis, and apoptosis.[68−70] Human cancer cells possess elevated levels of proteasome activity and are more sensitive to proteasome inhibitors than normal cells.[68] Proteasome inhibition bypasses, at least partly, the resistance of cancer cells to apoptosis because it activates macroautophagy, a compensatory protein degradation system,[71] and other pro-survival signaling pathways.[72] Inhibition of these autoprotective responses sensitizes cancer cells to the antiproliferative effects of proteasome inhibitors.[72] The proteasome inhibitor bortezomib (PS-341) was the first clinically available proteasome inhibitor and was approved by the FDA in 2003 for the treatment of

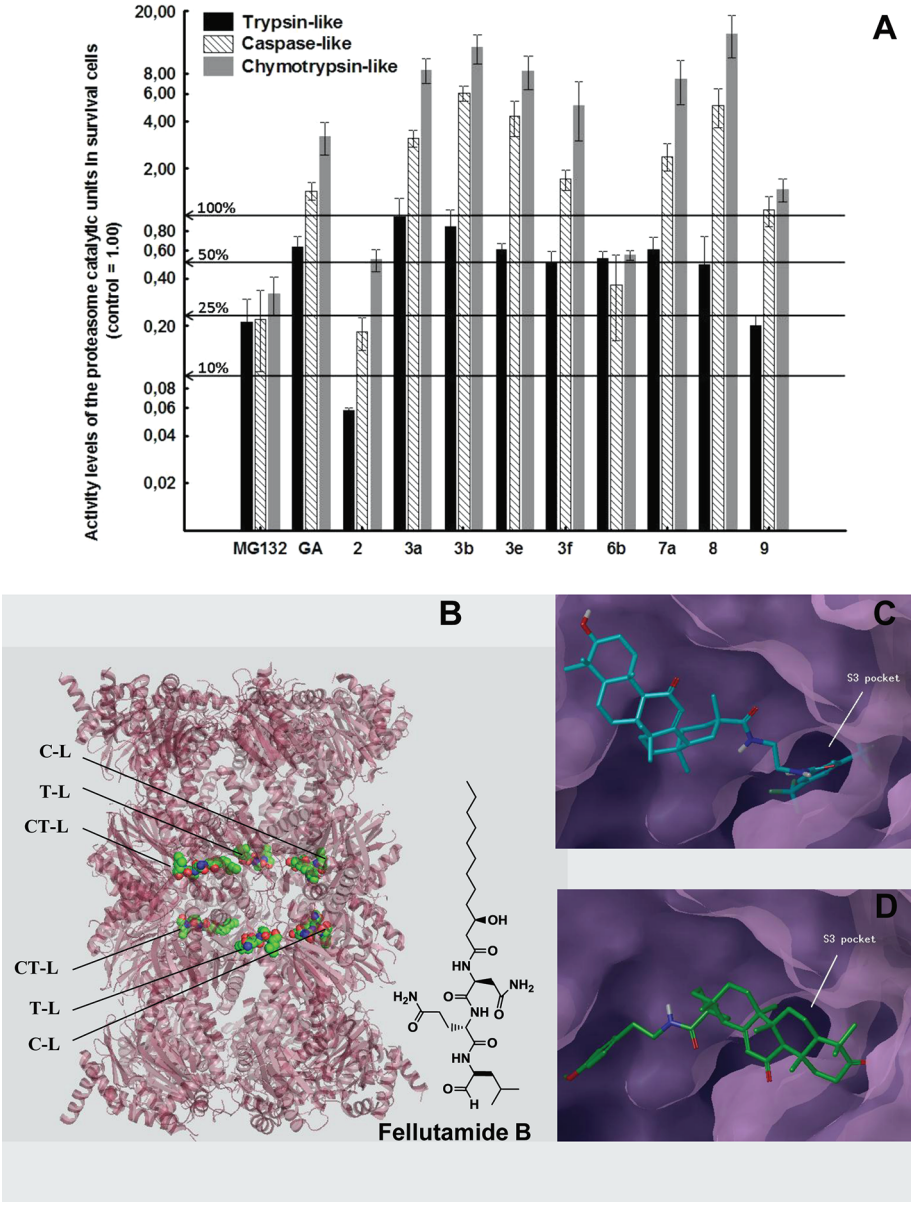

Figure 3. (A) Determination of the effects of the 10 compounds in this study on the proteolytic activity of the proteasome in human U373 GBM cells treated with each compound at their IC_{50} *in vitro* growth inhibitory concentrations, which are detailed in Table 1. MG-132 (0.5 μM) was used as a reference compound. The data are presented as mean ± SD values calculated in triplicate for each experimental condition. The *Y*-axis is on a logarithmic scale. (B) Ribbon representation of the 20S proteasome crystallographic structure bound to the fellutamide B ligand in the three pairs of binding sites (PDB code: 3D29): chymotrypsin-like sites (CT-L), trypsin-like sites (T-L), caspase-like sites (C-L). Fellutamide B is depicted as balls. (C,D) Comparison of the predicted best affinity binding modes of compounds **6b** (C) and **3e** (D) in the chymotrypsin-like site of the 3D29 crystal structure. The ligands are depicted as sticks and the protein is represented by its molecular surface. The S3 specificity pocket is indicated.

multiple myeloma.[73] However, despite clinical benefits, bortezomib causes various types of toxicities including peripheral neuropathy[74] and thrombocytopenia.[75]

The current study reveals that **1** inhibits the trypsine-like catalytic activity of the proteasome by ~50% while it activates the chymotrypsin-like catalytic activity. It also appears to be without any apparent effects on the caspase-like catalytic activity when tested at its IC_{50} *in vitro* growth inhibitory concentration (Figure 3A). The already known compound **2**,[27] i.e., *N*-(2-aminoethyl)-glycyrrhetinamide, behaved as a proteasome inhibitor, probably because of its amine function, which is well-known to have potent activity on cell viability (Table 1). In addition, its IC_{50} growth inhibitory concentrations in the eight cancer cell lines under study was similar to the one displayed by **1** (Table 1). The novel GA derivative **6b** (*N*-(2-{3-[3,5-bis(trifluoromethyl)phenyl]ureido}ethyl)-glycyrrhetinamide) was also able to inhibit the three catalytic units of the proteasome (Figure 3A). At first glance, **6b** appears to be less potent than **2** in its inhibitory activity toward the proteasome (Figure 3A). However, it should be noted that compound **6b** has been tested at a concentration of 7 μM (i.e., its IC_{50} *in vitro* growth inhibitory concentration; Table 1), whereas compound **2** has been tested at 60 μM (also its IC_{50} *in*

dx.doi.org/10.1021/jm200285z |*J. Med. Chem.* 2011, 54, 6501–6513

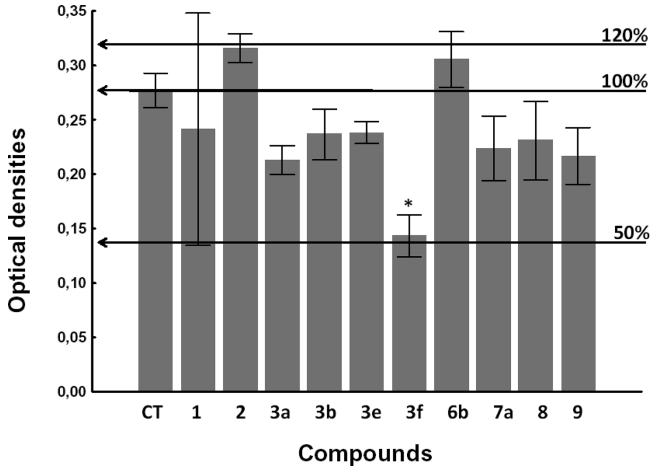

Figure 4. Determination of activating versus inhibiting effects of the 10 compounds in this study (the same as those used for proteasome-related studies; see Figure 3A) on PPAR-γ. Each compound has been analyzed at its IC_{50} in vitro growth inhibitory concentration in the human U373 GBM cell line (see Table 1 and its legend) treated for 6 h with the compound. The data are presented as mean ± SD values calculated in triplicate for each experimental condition. Determination of the effects of the 10 compounds after 6 h of treatment of human U373 GBM cells.

vitro growth inhibitory concentration; Table 1). Compound **6b** could therefore be considered as a novel GA derivative that acts both as a proteasome inhibitor and as a kinase inhibitor, as detailed below. It must be noticed that, apart from **2** and **6b**, the remaining compounds under study for which their effects on the proteasome have been analyzed display activating rather than inhibiting effects on the proteasome.

Before analyzing the antikinase profile of **6b**, we investigated its effects on PPARs because **1** and several of its derivatives can also target PPARs.[21−24] PPAR agonists, particularly thiazolidinedione derivatives, are promising therapeutic agents because they exert both a direct anticancer and a broad spectrum of antistromal, antiangiogenic, and immuno-modulating activities.[25,76] However, the great majority of reports from the literature clearly indicate that PPAR-targeting anticancer agents must display overall agonistic and not antagonistic activity for PPAR-γ.[77−80] Chintharlapalli et al.[21] and Jutooru et al.[15] demonstrated PPAR-γ activation with **1** derivatives in colon and pancreatic cancer cells, respectively. Thus, we wanted to confirm that **6b** does not antagonize PPAR-γ activity before further deciphering the mechanisms of action through which it displays its cytostatic activity in cancer cells. The data illustrated in Figure 4B confirm that **6b** (and also **2**) did not antagonize PPAR-γ activity, whereas the remaining compounds, including the reference compounds **8**[28] and **9**,[24] antagonized PPAR-γ activity when assayed at their IC_{50} *in vitro* growth inhibitory concentration (Table 1).

Together, these data thus highlight the fact that **6b**, which is a novel GA (**1**) derivative, displays marked *in vitro* activity both in apoptosis-resistant and apoptosis-sensitive cancer cells and that this cytostatic activity is partly mediated through the inhibition of the three catalytic units of the proteasome. As previously indicated in the Introduction, **1** and/or several **1** derivatives are also known to target various kinases, including the following: phosphatidylinositol-3-kinase (PI3−K) and p42 and p38 mitogen-activated protein kinase (MAPK),[15] src,[16] protein kinase C (PKC),[17] VEGF receptor 2 (VEGFR2), mTOR kinase, ribosomal S6 kinase (S6K),[18] and the PI3K/Akt/GSK3β pathway.[19] Kinase inhibitors are the largest class of new anticancer drugs,[81] and approximately 150 kinase inhibitors have been subjected to recent clinical testing, with ∼45 kinases listed as primary targets.[82] However, it is already apparent that most cancers can avoid the inhibition of any single kinase.[81] It becomes, in fact, increasingly obvious that it is mandatory to inhibit multiple kinases,[81] and partial inhibition of a small number of kinases appears to be a more promising strategy.[83] The data from the present study reveal that **6b** inhibits the activity of a dozen kinases, and most if not all of them are implicated in cancer cell proliferation and migration (see Table 2). It thus seems that the cytostatic activity of **6b** relates, at least partly, to the targeting of this cluster of kinases, a feature that was observed at 1 μM, which is a concentration ranging between 8% and 25% of the IC_{50} *in vitro* growth inhibitory concentrations determined in a panel of eight distinct cancer cell lines. These **6b**-mediated effects on kinases that are implicated in cancer cell proliferation and migration (with the implication of the actin cytoskeleton that also exerts major roles in cytokinesis, and thus in cell proliferation) can explain, at least partly, the **6b**-induced cytostatic effects.

In conclusion, the present study provides a novel **1** derivative, **6b**, which displays cytostatic and not cytotoxic effects in cancer cells. These cytostatic effects occur, at least partly, through the targeting of a limited number of 12 kinases that are implicated in cancer cell proliferation and migration and through antiproteasome activity, including the three catalytic units of the proteasome, while **6b** does not inhibit PPAR-γ activity in cancer cells. In contrast, **1** is less efficient than **6b** in inhibiting proteasome activity and it is cytotoxic, at least partly through the activation of pro-apoptotic processes. Compound **1**, i.e., glycyrrhetinic acid, displays *in vitro* growth inhibitory activity in various cancer cells with an efficiency that is about ten times weaker than that displayed by **6b**. We are currently developing specifically formulated forms of **6b** to proceed with *in vivo* experiments aimed at investigating the anticancer activity of **6b** as a single agent or in association with conventional cytotoxic chemotherapeutics.

EXPERIMENTAL SECTION

Chemistry. *General Methods.* Before their use, the solvents were distilled and dried using standard methods, i.e., THF and ether from Na/benzophenone, and CH_2Cl_2 from P_2O_5. The ^1H NMR and ^{13}C NMR spectra were recorded on a Bruker Avance 300 spectrometer in $CDCl_3$ using the residual isotopic solvent $CHCl_3$ and CH_3OH, respectively, as references for δ_H = 7.26 ppm, δ_C = 77.16 ppm, δ_H = 3.31 ppm, δ_C = 49.00 ppm. The following abbreviations are used for spin multiplicity: s, singlet; d, doublet; t, triplet; q, quadruplet, qt, quintuplet; m, multiplet; br, broad. ^1H NMR and ^{13}C NMR spectra were assigned by comparison with NMR spectra of oleanane compounds previously described in the literature.[84,85] Routine thin-layer chromatography (TLC) was performed on silica gel plates (Silica gel GF254 from VWR), and visualization was performed using UV. Flash column chromatography was carried out using silica gel at moderate pressure (spherical particle size 60−200 μm from MP Biomedicals). HPLC analyses were performed with an Agilent 1100 series HPLC system (Agilent, Diegem, Belgium). The chromatographic system was an RX-C8 (5 μm) (4.6 mm × 250 mm) (Agilent, Diegem, Belgium) using the same mobile phase for all compounds: MeOH−water 90:10 (0.1% TFA) 20 min. The detection system was an Agilent Diode Array Detector G1315B (monitoring wavelength given for each compound) (Agilent, Diegem, Belgium). The purity given was measured by this HPLC method at 249 nm. However, we are aware that this method does not take into account the

cocrystallized solvents that could be detected with NMR. High-resolution mass spectra (positive mode) were recorded by direct infusion in a 6520 series electrospray ion source (ESI)−quadrupole time-of-flight (Q-TOF) mass spectrometer (Agilent, Palo Alto, CA, USA). The error between the observed mass and the calculated mass is expressed in ppm. Below 3 ppm, the compounds were considered to have the predicted formula. The infrared spectra were recorded as KBr pellets on a Perkin-Elmer 1750 FT-spectrophotometer (Perkin-Elmer, Waltham, MA, USA) and the wavelengths are expressed in cm^{-1}. The monoprotected ethylenediamine, i.e., $H_2NCH_2CH_2NHBoc$, was synthesized according to procedures previously described in the literature.[29] The purity of each synthesized compound was verified by means of ^1H NMR, HRMS, and HPLC-UV analyses and reached a level >95% (Table 1).

*Procedure for the Synthesis of N-(2-Aminoethyl)-glycyrrhetinamide (**2**).* Compound **5** (450 mg, 0.735 mmol) was dissolved in DCM (9 mL) at 0 °C under stirring. Trifluoroacetic acid (1 mL, 13 mmol) was added, and the reaction was stirred at 0 °C for 3 h. The reaction mixture was evaporated below 50 °C and then poured into dry sodium bicarbonate and ice, extracted with dichloromethane, dried over Na_2SO_4, filtered, and concentrated to produce the corresponding amine in quantitative yield.

*General Procedure for 18 β-Glycyrrhetinamides (**3**, **5**).* 18-β-Glycyrrhetinic acid (200 mg, 0.43 mmol) was dissolved in DMF (10 mL) at room temperature under stirring. *N,N′*-Dicyclohexylcarbodiimide (175.3 mg, 0.85 mmol), 1-hydroxy-1*H*-benzotriazole (86.1 mg, 0.64 mmol), and diisopropylethylamine (444 μL, 2.55 mmol) were added successively to the reaction mixture. After 30 min, the solution was cooled at 0 °C, and the primary amine was added dropwise. The reaction mixture was brought to room temperature and then was stirred overnight. The reaction mixture was concentrated under vacuum and water was added. After dichloromethane extraction, the organic layer was dried over anhydrous Na_2SO_4, filtered, and concentrated under vacuum. *N,N′*-Dicyclourea was eliminated by trituration in acetonitrile. The organic layer was evaporated under vacuum. The crude product was then chromatographed on silica (cyclohexane; ethyl acetate).

*Procedure for the Synthesis of **3e** from **3d**.* Compound **3d** (200 mg, 0.331 mmol) was dissolved in acetone (20 mL) at 0 °C under stirring. Jones reagent (150 μL) was added dropwise until the reaction mixture became orange. After 45 min, methanol was added until the solution turned dark green. The reaction was poured into a mixture of ice and water (20 mL), and then acetone and methanol were removed under reduced pressure. The aqueous residue was extracted three times with 10 mL DCM. The combined organic extracts were washed first with water (10 mL) and then with brine (10 mL) and dried over Na_2SO_4. The solvent was evaporated under vacuum, leading to a solid that corresponds to compound **3e** (98% yield).

*General Procedure for 18 β-Glycyrrhetindiamides (**4**).* Compound **2** (100.8 mg, 0.20 mmol) was dissolved in 4 mL of anhydrous DCM. *N,N′*-Dimethylaminopyridine (48.7 mg, 0.40 mmol) was then added to this solution. After cooling at 0 °C, the acyl chloride (0.20 mmol) was added dropwise to the reaction mixture, which was then stirred at room temperature for 12 h. The mixture was concentrated under vacuum. The residual solid was dissolved in 20 mL of DCM and the organic layer was washed twice with 20 mL of 1 M HCl. The aqueous layer was then extracted twice with 10 mL of DCM. The combined organic layers were washed twice with 20 mL of 1 M NaOH, and the aqueous layers were extracted twice with 10 mL of DCM. The combined organic layers were dried over anhydrous Na_2SO_4, filtered, and concentrated under reduced pressure. The crude product was then chromatographed on silica (DCM; methanol).

*General Procedure for (Thio)Ureido-glycyrrhetinamides (**6**, **7**).* Compound **2** (90.9 mg, 0.18 mmol) was dissolved in 4 mL of anhydrous THF. The desired isocyanate or thioisocyanate (0.18 mmol) was added. The reaction mixture was stirred at room temperature for 20 h and was concentrated under vacuum. The residual solid was then chromatographed on silica (DCM; methanol), with the exception of compounds **6b** and **7b**, which were purified through trituration in Et_2O.

*N-(2-{3-[3,5-Bis(trifluoromethyl)phenyl]ureido}ethyl)-glycyrrhetinamide (**6b**).* Yield: 36%. Rf = 0.30 (DCM; MeOH 95:5). RP-HPLC: purity = 99%, t_R = 8.40 min ^1H NMR characteristic protons (HSQC, 300 MHz, CD_3OD): δ (ppm) = 8.02 (s, 2H, Ar−H35, H39), 7.42 (s, 1H, Ar-H37), 5.61 (s, 1H, CH-12), 3.62−3.22 (m, 4H, $NHCH_2CH_2NH$), 3.15 (dd, 1H, *J* = 7.0 Hz, 5.1 Hz, CH-3), 2.66 (dt, 1H, *J* = 13.0 Hz, 3.0 Hz, CH-1), 2.37 (s, 1H, CH-9), 1.38 (s, 3H, Me-H27), 1.10 (s, 3H, Me-H29), 1.05 (s, 3H, Me-H25), 0.98 (s, 3H, Me-H23), 0.94 (s, 3H, Me-H26), 0.78 (s, 3H, Me-H24), 0.74 (s, 3H, Me-H28). ^{13}C NMR (HSQC, 75 MHz, CD_3OD): δ (ppm) = 202.4 (C11), 179.4 (C30), 172.6 (C13), 157.6 (C33), 143.4 (C34), 133.0 (q, *J* = 33.0 Hz, C36/C38), 128.9 (C12), 124.8 (q, *J* = 270.1 Hz, CF_3), 118.8 (q, *J* = 3.0 Hz, C35/C39), 115.3 (q, *J* = 7.0 Hz, C37), 79.4 (C3), 63.1 (C9), 56.2 (C5), 49.3 (C18), 46.6 (C14), 44.9 (C20), 44.5 (C8), 42.6 (C19), 41.1 (C31/C32*), 40.6 (C31/C32*), 40.3 (C1), 40.2 (C4), 38.7 (C22), 38.3 (C10), 33.7 (C7), 32.9 (C17), 31.9 (C21), 29.6 (C29), 29.1 (C28), 28.7(C23), 27.8 (C2), 27.6 (C15/C16*), 27.4 (C15/C16*), 23.7 (C27), 19.1 (C26), 18.6 (C6), 16.8 (C25), 16.3 (C24). IR (KBr): ν (cm^{-1}): 3360 (OH), 2932 (CH aliphatic), 1643 (C═O), 1544, 1467, 1386. Mp: 201 °C. HRMS (ESI-QTOF) calcd for (**6b**) $C_{41}H_{55}F_6N_3O_4$ ($M+H^+$) 768.4170, obsd 768.4167, error: 0.29 ppm.

Pharmacology. *Determination of in Vitro Anticancer Activity.* The histological types and origin of the eight cancer cell lines are detailed in the legend of Table 1. The cells were cultured in RPMI (Invitrogen, Merelbeke, Belgium) media supplemented with 10% heat inactivated fetal calf serum (Invitrogen). All culture media were supplemented with 4 mM glutamine, 100 μg/mL gentamicin, and penicillin−streptomycin (200 U/mL and 200 μg/mL) (Invitrogen).

The overall growth level of human cancer cell lines was determined using a colorimetric MTT (3-[4,5-dimethylthiazol-2yl-diphenyl tetrazolium bromide, Sigma, Belgium) assay as detailed previously.[30−33] Each experimental condition was performed in six replicates.

Molecular Docking. Docking was conducted using the *Glide* program (version 4.5),[86] which positions the 3D structure of flexible ligands in the 3D structure of rigid or partially flexible receptors.

Docking experiments were performed on the X-ray crystallographic structure of the 20S proteasome from *Saccharomyces cerevisae* (PDB code 3D29).[51] The 20S proteasome is highly conserved from yeast to human.[87] The protein structures were prepared using the Protein Preparation Wizard in the Schrödinger software graphical user interface Maestro. Glide XP docking protocol and scoring function were used to dock in the rigid receptors and to score the poses of the different ligands. The default settings of *Glide* version 4.5 were used for the remaining parameters. For each docking run, the binding zone was defined as a cube of length 40 Å. This cube was centered on the former positions of the removed ligand cocrystallized with the protein in each proteolytic site. The initial 3D structures of the ligands were generated with the *CORINA* program.[88]

Biochemical Analyses Aimed at Characterizing Anti-Proteasome Activity. The substrates used for performing this assay were Suc-LLVY-Glo, Z-LRR-Glo, and Z-nLPnLD-Glo for the chymotrypsin-like, trypsin-like, and caspase-like assay, respectively. U373 GBM cells were incubated at a concentration of 5000 cells/mL for 48 h in three different 96-microwell plates (one plate for each catalytic site). U373 GBM cells were then treated with each compound at their IC_{50} *in vitro* growth inhibitory concentration (see Table 1) for two days. Cells were then washed with PBS (Invitrogen, Merelbeke, Belgium) before adding digitonin at 0.025% to rapidly and selectively permeate the cytoplasmic membranes.[89] Proteasome-Glo reagent (Promega Corporation, USA), specific for a catalytic site, was added in each well sample. Because the light of the aminoluciferine released was proportional to the rate of

proteasome cleavage of the substrate, after 10 min of dark incubation, the bioluminescence of each well was measured with an ActiveGlo LR-100 luminometer (DSLabs, USA). Each experiment was conducted in triplicate. These cells' bioluminescence assay was normalized by a concomitant cell viability assay (using the MTT colorimetric assay as detailed before) performed using strictly identical conditions.

PPAR-γ Activity Assay. U373 glioblastoma cells were treated with each compound at their IC_{50} *in vitro* growth inhibitory concentration (see Figure 4 and its legend) for 6 h. After these incubations, cells were collected and nuclear extracts were purified according to the manufacturer's instructions (Cayman Chemical; Complete Transcription Factor Assay Kit). In brief, cells were detached with trypsin and centrifuged at 300 g for 5 min. The pellets were resuspended in an ice-cold PBS/Phosphatase inhibitor solution for 5 min. This step was repeated once. Extracts were resuspended in ice-cold hypotonic buffer and incubated for 15 min. To break the cytoplasmic membrane, cells were treated with Nonidet p-40 (Sigma-Aldrich, Bornem, Belgium). The extracts were centrifuged and the cytoplasmic fraction was saved for other applications. The pellet was resuspended in an extraction buffer containing protease inhibitor and incubated with gentle rocking for 30 min on ice. Extracts were centrifuged at 14 000 *g* for 10 min at 4 °C. The supernatant contained the nuclear fraction. Nuclear extracts were loaded in 96 well plates and incubated overnight at 4 °C. The primary antibody (from the PPAR-γ; Complete Transcription Factor Assay Kit) was added and incubated for one hour at room temperature. The wells were washed 5 times and a goat antirabbit HRP conjugated secondary antibody was added and incubated for one hour at room temperature. The wells were washed 5 times. Developing solution was added for 45 min and absorbance was measured at 450 nm with a spectrophotometer (Biorad model 680XR, Biorad, Nazareth, Belgium).

Flow Cytometry Determination of Apoptosis and Cell Cycle Kinetics. Analyses of apoptosis and cell cycle kinetics were performed with the APO AF detection kit (BD Pharmingen, Erembodegem-Aalst, Belgium) according to the manufacturer's instructions and based on a procedure we previously described.[36] The cancer cells were treated for 48 or 72 h with their respective IC_{50} *in vitro* growth inhibitory concentrations, 10 μM for U373 and A549 cancer cells (**6b**), and 80 and 100 μM for U373 and A549 cancer cells (**1**). TUNEL labeling of U373 GBM and A549 NSCLC cells was performed for 1 h at 37 °C followed by propidium iodide (PI) staining (5 μg/mL) in the presence of RNase. Stained cells were analyzed on a CellLab Quanta SC flow cytometer (Beckman Coulter; Analis, Suarlee, Belgium).

Kinase Activity Determination. We originally prepared ProQinase (Freiburg, Germany) with **6b** as a stock solution in 100% DMSO, and aliquots were further diluted with water in 96 well microliter plates immediately before use. For each kinase assay, 5 μL from a 2×10^5 M/10% DMSO compound solution were transferred into the assay plates. The final volume of the assay was 50 μL. The final assay concentration of **6b** was 1 μM. A radiometric protein kinase assay (^{33}PanQinase Activity Assay) was used to measure the kinase activity of the 333 protein kinases under study, as detailed previously.[90]

Statistical Analyses. Data obtained from independent groups were compared by the nonparametric Kruskal−Wallis (Dunn's procedure), Mann−Whitney U, or Spearman Rank Correlation tests. The statistical analysis was performed using *Statistica* software (Statsoft, Tulsa, OK).

■ ASSOCIATED CONTENT

Supporting Information. The characterization data for all compounds that have been synthesized and biologically evaluated in this study (HPLC, ^{1}H NMR, ^{13}C NMR, mass spectra, etc.) and the detailed biological and biochemical protocols.This material is available free of charge via the Internet at http://pubs.acs.org.

■ AUTHOR INFORMATION

Corresponding Author
*Tel.: +32 477 62 20 83; E-mail: rkiss@ulb.ac.be.

■ ACKNOWLEDGMENT

Q-TOF was acquired thanks to grants from the Fonds National de la Recherche Scientifique (FRS-FNRS) no 34553.08 and from the Université Libre de Bruxelles (ULB-FER2007). Marina Bury is the holder of a grant FRIA from the FNRS and Cédric Delporte is a PhD student from the FNRS. Robert Kiss is a director of research with the FNRS. Jean-Paul Becker is a postdoctoral fellow supported by the F.R.S.-FNRS. Martine Prévost is 'Maître de Recherche' at the FNRS. We thank Prof. M. Luhmer and Dr. R. D'Orazio from CIREM (ULB) for NMR spectra recording, Dr. P. Van Antwerpen for the HRMS analysis from Analytical Platform of the Pharmacy Faculty (ULB), and V. Megalizzi for the setting up of the proteasome test.

■ ABBREVIATIONS

ATCC: American Type Culture Collection; DSMZ: Deutsche Sammlung von Mikroorganismen and Zellkulturen; ECACC: European Collection of Cell Culture; GA: Glycyrrhetinic acid; GBM: Glioblastoma; MTT: 3-(4,5)-Dimethylthiazol-2-yl)-2,5-diphenyl-tetrazolium bromide; NSCLC: Non-small-cell lung carcinoma; PPARs: Peroxysome proliferator-activated receptors

■ REFERENCES

(1) Obolentseva, G. V.; Litvinenko, V. I.; Ammosov, A. S.; Popova, T. P.; Sampiev, A. M. Pharmacological and therapeutic properties of licorice preparations. *Pharm. Chem. J.* **1999**, *33*, 427–434.

(2) Abe, H.; Ohya, N.; Yamamoto, K. F.; Shibuya, T.; Arichi, S.; Odashima, S. Effects of glycyrrhizin and glycyrrhetinic acid on growth and melanogenesis in cultured B16 melanoma cells. *Eur. J. Cancer Clin. Oncol.* **1987**, *23*, 1549–1555.

(3) Okamoto, H.; Yoshida, D.; Mizusaki, S. Inhibition of 12-O-tetradecanoylphorbol-13-acetate-induced induction in Epstein-Barr virus early antigen in Raji cells. *Cancer Lett.* **1983**, *19*, 47–53.

(4) Hibasami, H.; Iwase, H.; Yoshioka, K.; Takahashi, H. Glycyrrhetic acid (a metabolic substance and aglycon of glycyrrhizin) induces apoptosis in human hepatoma, promyelotic leukemia and stomach cancer cells. *Int. J. Mol. Med.* **2006**, *17*, 215–219.

(5) Isbrucker, R. A.; Burdock, G. A. Risk and safety assessment on the consumption of licorice root (Glycyrrhiza sp.), its extract and powder as a food ingredient, with emphasis on the pharmacology and toxicology of glycyrrhizin. *Regul. Toxicol. Pharmacol.* **2006**, *46*, 167–192.

(6) Zhang, M.-Z.; Xu, J.; Yao, B.; Yin, H.; Cai, Q.; Shrubsole, M. J.; Chen, X.; Kon, V.; Zheng, W.; Pozzi, A.; Harris, R. C. Inhibition of 11beta-hydroxysteroid dehydrogenase type II selectively blocks the tumor COX-2 pathway and suppresses colon carcinogenesis in mice and humans. *J. Clin. Invest.* **2009**, *119*, 876–885.

(7) Satomi, Y.; Nishino, H.; Shibata, S. Glycyrrhetinic acid and related compounds induce G1 arrest and apoptosis in human hepatocellular carcinoma HepG2. *Anticancer Res.* **2005**, *25*, 4043–4047.

(8) Hawthorne, S.; Gallagher, S. Effects of glycyrrhetinic acid and liquorice extract on cell proliferation and prostate-specific antigen secretion in LNCaP prostate cancer cells. *J. Pharm. Pharmacol.* **2008**, *60*, 661–666.

(9) Lee, C. S.; Yang, J. C.; Kim, Y. J.; Jang, E. R.; Kim, W.; Myung, S. C. 18beta-glycyrrhetinic acid potentiates apoptotic effect of trichostatin A on human epithelial ovarian carcinoma cell lines. *Eur. J. Pharmacol.* **2010**, *649*, 354–361.

(10) Salvi, M.; Fiore, C.; Armanini, D.; Toninello, A. Glycyrrhetinic acid-induced permeability transition in rat liver mitochondria. *Biochem. Pharmacol.* **2003**, *66*, 2375–2379.

(11) Lee, C. S.; Kim, Y. J.; Lee, M. S.; Han, E. S.; Lee, S. J. 18beta-Glycyrrhetinic acid induces apoptotic cell death in SiHa cells and exhibits a synergistic effect against antibiotic anti-cancer drug toxicity. *Life Sci.* **2008**, *83*, 481–489.

(12) Schwarz, S.; Csuk, R. Synthesis and antitumour activity of glycyrrhetinic acid derivatives. *Bioorg. Med. Chem.* **2010**, *18*, 7458–7474.

(13) Anuchapreeda, S.; Leechanachai, P.; Smith, M. M.; Ambudkar, S. V.; Limtrakul, P. N. Modulation of P-glycoprotein expression and function by curcumin in multidrug-resistant human KB cells. *Biochem. Pharmacol.* **2002**, *64*, 573–582.

(14) Mayur, Y. C.; Peters, G. J.; Prasad, V. V.; Lemo, C.; Sathish, N. K. Design of new drug molecules to be used in reversing multidrug resistance in cancer cells. *Curr. Cancer Drug Targets* **2009**, *9*, 298–306.

(15) Jutooru, I.; Chadalapaka, G.; Chintharlapalli, S.; Papineni, S.; Safe, S. Induction of apoptosis and nonsteroidal anti-inflammatory drug-activated gene 1 in pancreatic cancer cells by a glycyrrhetinic acid derivative. *Mol. Carcinog.* **2009**, *48*, 692–702.

(16) Chung, T. H.; Wang, S. M.; Chang, Y. C.; Chen, Y. L.; Wu, J. C. 18beta-glycyrrhetinic acid promotes src interaction with connexin43 in rat cardiomyocytes. *J. Cell Biochem.* **2007**, *100*, 653–664.

(17) Kawakami, Z.; Ikarashi, Y.; Kase, Y. Glycyrrhizin and its metabolite 18beta-glycyrrhetinic acid in glycyrrhiza, a constituent herb of yokukansan, ameliorate thiamine deficiency-induced dysfunction of glutamate transport in cultured rat cortical astrocytes. *Eur. J. Pharmacol.* **2010**, *626*, 154–158.

(18) Pang, X.; Zhang, L.; Wu, Y.; Lin, L.; Li, J.; Qu, W.; Safe, S.; Liu, M. Methyl 2-cyano-3,11-dioxo-18-olean-1,12-dien-30-oate (CDODA-Me), a derivative of glycyrrhetinic acid, functions as a potent angiogenesis inhibitor. *J. Pharmacol. Exp. Ther.* **2010**, *335*, 172–179.

(19) Kao, T.; Shyu, M. H.; Yen, G. C. Glycyrrhizic acid and 18beta-glycyrrhetinic acid inhibit inflammation via PI3K/Akt/GSK3beta signaling and glucocorticoid receptor activation. *J. Agric. Food Chem.* **2010**, *58*, 8623–8629.

(20) Huang, L.; Yu, D.; Ho, P.; Qian, K.; Lee, K. H.; Chen, C. H. Synthesis and proteasome inhibition of glycyrrhetinic acid derivatives. *Bioorg. Med. Chem.* **2008**, *16*, 6696–6701.

(21) Chintharlapalli, S.; Papineni, S.; Jutooru, I.; McAlees, A.; Safe, S. Structure-dependent activity of glycyrrhetinic acid derivatives as peroxisome proliferator-activated receptor gamma agonists in colon cancer cells. *Mol. Cancer Ther.* **2007**, *6*, 1588–1598.

(22) Chintharlapalli, S.; Papineni, S.; Konopleva, M.; Andreef, M.; Samudio, I.; Safe, S. 2-cyano-3,12-dioxoolean-1,9-dien-28-oic acid and related compounds inhibit growth of colon cancer cells through peroxisome proliferator-activated receptor gamma-dependent and -independent pathways. *Mol. Pharmacol.* **2005**, *68*, 119–128.

(23) Papineni, S.; Chintharlapalli, S.; Safe, S. Methyl 2-cyano-3,11-dioxo-18beta -olean-1,12-dien-30-oate is a peroxisome proliferator-activated receptor-gamma agonist that induces receptor-independent apoptosis in LNCaP prostate cancer cells. *Mol. Pharmacol.* **2008**, *73*, 553–565.

(24) Chadalapaka, G.; Jutooru, I.; McAlees, A.; Stefanac, T.; Safe, S. Structure-dependent inhibition of bladder and pancreatic cancer cell growth by 2-substituted glycyrrhetinic and ursolic acid derivatives. *Bioorg. Med. Chem. Lett.* **2008**, *18*, 2633–2639.

(25) Michalik, L.; Wahli, W. PPARs mediate lipid signaling in inflammation and cancer. *PPAR Res.* **2008**, ID 134059, doi:10.1155/2008/134059.

(26) Bundscherer, A.; Reichle, A.; Hafner, C.; Meyer, S.; Vogt, T. Targeting the tumor stroma with peroxisome proliferator activated receptor (PPAR) agonists. *Anticancer Agents Med. Chem.* **2009**, *9*, 816–821.

(27) He, X.; Yu, S.; Dong, Y. Y.; Yan, F.; Chen, L. Preparation and properties of a novel thermo-responsive poly(N-isopropylacrylamide) hydrogel containing glycyrrhetinic acid. *J. Mater. Sci.* **2009**, *44*, 4078–4086.

(28) Tatsuzaki, J.; Taniguchi, M.; Bastow, K. F.; Nakagawa-Goto, K.; Morris-Natschke, S. L.; Itokawa, H.; Baba, K.; Lee, K.-H. Anti-tumor agents: Novel glycyrrhetinic acid-dehydrozingerone conjugates as cytotoxic agents. *Bioorg. Med. Chem.* **2007**, *15*, 6193–6199.

(29) Fukuoka, S.; Kida, T.; Nakajima, Y.; Tsumagari, T.; Watanabe, W.; Inaba, Y.; Mori, A.; Matsumura, T.; Nakano, Y.; Takeshita, K. Thermo-responsive extraction of cadmium(II) ion with TPEN-NIPA gel. Effect of the number of polymerizable double bond toward gel formation and the extracting behavior. *Tetrahedron* **2010**, *66*, 1721–1727.

(30) Joseph, B.; Darro, F.; Béliard, A.; Lesur, B.; Collignon, F.; Decaestecker, C.; Frydman, A.; Guillaumet, G.; Kiss, R. 3-aryl-2-quinolone derivatives: synthesis and characterization of *in vitro* and *in vivo* anti-tumor effects with emphasis on a new therapeutical target connected with cell migration. *J. Med. Chem.* **2002**, *45*, 2543–2555.

(31) Ozap-Yaman, S.; de Hoog, P.; Amadei, G.; Pitié, M.; Gamez, P.; Dewelle, J.; Mijatovic, T.; Meunier, B.; Kiss, R.; Reedijk, J. Platined copper (3-clip-phen) complexes as effective DNA-cleaving and cytotoxic agents. *Chem.—Eur. J.* **2008**, *14*, 3418–3426.

(32) Lamoral-Theys, D.; Andolfi, A.; Van Goietsenoven, G.; Cimmino, A.; Le Calvé, B.; Wauthoz, N.; Mégalizzi, V.; Gras, T.; Bruyère, C.; Dubois, J.; Mathieu, V.; Kornienko, A.; Kiss, R.; Evidente, A. Lycorine, the main phenanthridine Amaryllidaceae alkaloid, exhibits significant antitumor activity in cancer cells that display resistance to proapoptotic stimuli: An investigation of structure-activity relationship and mechanistic insight. *J. Med. Chem.* **2009**, *52*, 6244–6256.

(33) Ingrassia, L.; Lefranc, F.; Dewelle, J.; Pottier, L.; Mathieu, V.; Spiegl-Kreinecker, S.; Sauvage, S.; El Yazidi, M.; Dehoux, M.; Berger, W.; Van Quaquebeke, E.; Kiss, R. Structure-activity relationship analysis of novel derivatives of narciclasine (an Amaryllidaceae isocarbostyril derivative) as potential anticancer agents. *J. Med. Chem.* **2009**, *52*, 1100–1114.

(34) Branle, F.; Lefranc, F.; Camby, I.; Jeuken, J.; Geurts-Moespot, A.; Sprenger, S.; Sweep, F.; Kiss, R.; Salmon, I. Evaluation of the efficiency of chemotherapy in *in vivo* orthotopic models of human glioma cells with and without 1p19q deletions and in C6 rat orthotopic allografts serving for the evaluation of surgery combined with chemotherapy. *Cancer* **2002**, *95*, 641–655.

(35) Mathieu, A.; Remmelink, M.; D'Haene, N.; Penant, S.; Gaussin, J. F.; Van Ginckel, R.; Darro, F.; Kiss, R.; Salmon, I. Development of a chemoresistant orthotopic human nonsmall cell lung carcinoma model in nude mice. *Cancer* **2004**, *101*, 1908–1918.

(36) Mijatovic, T.; Mathieu, V.; Gaussin, J. F.; De Nève, N.; Ribaucour, F.; Van Quaquebeke, E.; Dumont, P.; Darro, F.; Kiss, R. Cardenolide-induced lysosomal membrane permeabilization demonstrates therapeutic benefits in experimental human non-small cell lung cancers. *Neoplasia* **2006**, *5*, 402–412.

(37) Mathieu, V.; Pirker, C.; Martin de Lassalle, E.; Vernier, M.; Mijatovic, T.; De Neve, N.; Gaussin, J. F.; Dehoux, M.; Lefranc, F.; Berger, W.; Kiss, R. The sodium pump alpha-1 subunit: a disease progression-related target for metastatic melanoma treatment. *J. Cell Mol. Med.* **2009**, *13*, 3960–3972.

(38) Dumont, P.; Ingrassia, L.; Rouzeau, S.; Ribaucour, F.; Thomas, S.; Roland, I.; Darro, F.; Lefranc, F.; Kiss, R. The *Amaryllidaceae* isocarbostyril narciclasine induces apoptosis by activation of the death receptor and/or mitochondrial pathways in cancer cells but not in normal fibroblasts. *Neoplasia* **2007**, *9*, 766–776.

(39) Gerber, D. E.; Minna, J. D. ALK inhibition for non-small cell lung cancer: from discovery to therapy in record time. *Cancer Cell* **2010**, *18*, 548–551.

(40) Qiu, Y.; Kung, H. J. Signaling network of the Btk family kinases. *Oncogene* **2000**, *19*, 5651–5661.

(41) Dopeso, H.; Mateo-Lozano, S.; Mazzolini, R.; Rodrigues, P.; Lagares-Tena, L.; Ceron, J.; Romero, J.; Esteves, M.; Landolfi, S.; Hernandez-Losa, J.; Castano, J.; Wilson, A. J.; Ramon y Cajal, S.; Mariadason, J. M.; Schwartz, S., Jr.; Arango, D. The receptor tyrosine kinase EPHB4 has tumor suppressor activities in intestinal tumorigenesis. *Cancer Res.* **2009**, *69*, 7430–7438.

(42) Herath, N. I.; Boyd, A. W. The role of Eph receptors and ephrin ligands in colorectal cancer. *Int. J. Cancer* **2010**, *126*, 2003–2011.
(43) Smith, J. A.; Samayawardhena, L. A.; Craig, A. W. Fps/Fes protein-tyrosine kinase regulats mast cell adhesion and migration dowstrean of kit and beta1 integrin receptors. *Cell Signal* **2010**, *22*, 427–436.
(44) Saito, Y. D.; Jensen, A. R.; Salgia, R.; Posadas, E. M. Fyn: a novel molecular target in cancer. *Cancer* **2010**, *116*, 1629–1637.
(45) Katoh, M. FGFR2 abnormalities underlies a spectrum of bone, skin, and cancer pathologies. *J. Invest. Dermatol.* **2009**, *129*, 1861–1867.
(46) Scartozzi, M.; Bianconi, M.; Maccaroni, E.; Giamperi, R.; Beradi, R.; Cascinu, S. Dalotuzumab, a recombinant humanized mAb targeted against IGFR1 for the treatment of cancer. *Curr. Opin. Mol. Ther.* **2010**, *12*, 361–371.
(47) Cockburn, J. G.; Richardson, D. S.; Gujral, T. S.; Mulligan, L. M. RET-mediated cell adhesion and migration require multiple integrin subunits. *J. Clin. Endocrinol. Metab.* **2010**, *95*, E342–E346.
(48) Lee, B. C.; Lee, T. H.; Zagozdzon, R.; Avraham, S.; Usheva, A.; Avraham, H. K. Carboxyl-terminal Src kinase homologous kinase negatively regulates the chemokine receptor CXCR4 through YY1 and impairs CXCR4/CXCL12 (SDF-1alpha)-mediated breast cancer cell migration. *Cancer Res.* **2005**, *65*, 2840–2845.
(49) Coniglio, S. J.; Zavarella, S.; Symons, M. H. Pak1 and Pak2 mediate tumor cell invasion through distinct signaling mechanisms. *Mol. Cell. Biol.* **2008**, *28*, 4162–4172.
(50) Lee, D. H.; Goldberg, A. L. Proteasome inhibitors: valuable new tools for cell biologists. *Trends Cell Biol.* **1998**, *8*, 397–403.
(51) Hines, J.; Groll, M.; Fahnestock, M.; Crews, C. M. Proteasome Inhibition by Fellutamide B Induces Nerve Growth Factor Synthesis. *Chem. Biol. (Cambridge, MA, U. S.)* **2008**, *15*, 501–512.
(52) de Bettignies, G.; Coux, O. Proteasome inhibitors: Dozens of molecules and still counting. *Biochimie* **2010**, *92*, 1530–1545.
(53) Blackburn, C.; Gigstad, K. M.; Hales, P.; Garcia, K.; Jones, M.; Bruzzese, F. J.; Barrett, C.; Liu, J. X.; Soucy, T. A.; Sappal, D. S.; Bump, N.; Olhava, E. J.; Fleming, P.; Dick, L. R.; Tsu, C.; Sintchak, M. D.; Blank, J. L. Characterization of a new series of non-covalent proteasome inhibitors with exquisite potency and selectivity for the 20S beta 5-subunit. *Biochem. J.* **2010**, *430*, 461–476.
(54) Geurink, P. P.; Liu, N.; Spaans, M. P.; Downey, S. L.; van den Nieuwendijk, A. M. C. H.; van der Marel, G. A.; Kisselev, A. F.; Florea, B. I.; Overkleeft, H. S. Incorporation of fluorinated phenylalanine generates highly specific inhibitor of proteasome's chymotrypsin-like sites. *J. Med. Chem.* **2010**, *53*, 2319–2323.
(55) Furet, P.; Imbach, P.; Noorani, M.; Koeppler, J.; Laumen, K.; Lang, M.; Guagnano, V.; Fuerst, P.; Roesel, J.; Zimmermann, J.; Garcia Echeverria, C. Entry into a new class of potent proteasome inhibitors having high antiproliferative activity by structure-based design. *J. Med. Chem.* **2004**, *47*, 4810–4813.
(56) Simpson, C. D.; Anyiwe, K.; Schimmer, A. D. Anoikis resistance and tumor metastasis. *Cancer Lett.* **2008**, *272*, 177–185.
(57) Savage, P.; Stebbing, J.; Bower, M.; Crook, T. Why does cytotoxic chemotherapy cure only some cancers? *Nat. Clin. Pract. Oncol.* **2009**, *6*, 43–52.
(58) Wilson, T. R.; Johnston, P. G.; Longley, D. B. Anti-apoptotic mechanisms of drug resistance in cancer. *Curr. Cancer Drug Targets* **2009**, *9*, 307–319.
(59) Bozec, A.; Peyrade, F.; Fischel, J. L.; Milano, G. Emerging molecular targeted therapies in the treatment of head and neck cancer. *Expert Opin. Emerg. Drugs* **2009**, *14*, 299–310.
(60) Han, S.; Roman, J. Targeting apoptotic signaling pathways in human lung cancer. *Curr. Cancer Drug Targets* **2010**in press.
(61) Soengas, M. S.; Lowe, S. W. Apoptosis and melanoma chemoresistance. *Oncogene* **2003**, *22*, 3138–3151.
(62) Wong, H. H.; Lemoine, N. R. Pancreatic cancer: molecular pathogenesis and new therapeutic targets. *Nat. Rev. Gastroenterol. Hepatol.* **2009**, *6*, 412–422.
(63) D'Amico, T. A.; Harpole, D. H., Jr. Molecular biology of esophageal cancer. *Chest Surg. Clin. N. Am.* **2000**, *10*, 451–469.
(64) Bruyère, C.; Lonez, C.; Duray, A.; Cludts, S.; Ruysschaert, J. M.; Saussez, S.; Yeaton, P.; Kiss, R.; Mijatovic, T. Considering Temozolomide as a novel potential treatment for oesophageal cancer. *Cancer* **2011**, *117*, 2004–2016.
(65) Lefranc, F.; Brotchi, J.; Kiss, R. Possible future issues in the treatment of glioblastomas, with a special emphasis on cell migration and the resistance of migrating glioblastoma cells to apoptosis. *J. Clin. Oncol.* **2005**, *23*, 2411–2422.
(66) Landis-Piwowar, K. R.; Milacic, V.; Chen, D.; Yang, H.; Zhao, Y.; Chan, T. H.; Yan, B.; Dou, Q. P. The proteasome as a potential target for novel anticancer drugs and chemosensitizers. *Drug Resist. Updates* **2006**, *9*, 263–273.
(67) Guo, L.; Zhou, Y.; Sun, Y.; Zhang, F. Non-receptor tyrosine kinase Etk regulation of drug resistance in small-cell lung cancer. *Eur. J. Cancer* **2010**, *46*, 636–641.
(68) Chen, D.; Dou, Q. P. The ubiquitin-proteasome system as a prospective molecular target for cancer treatment and prevention. *Curr. Protein Pept. Sci.* **2010**, *11*, 459–470.
(69) Tsukamoto, S.; Yokosawa, H. Targeting the proteasome pathway. *Expert Opin. Ther. Targets* **2009**, *13*, 605–621.
(70) Liggett, A.; Crawford, L. J.; Walker, B.; Morris, T. C. M.; Irvine, A. E. Methods for measuring proteasome activity: Current limitations and future developments. *Leukemia Res.* **2010**, *34*, 1403–1409.
(71) Lefranc, F.; Facchini, V.; Kiss, R. Pro-autophagic drugs: A novel means to combat apoptosis-resistant cancers, with a special emphasis on glioblastomas. *Oncologist* **2007**, *12*, 1395–1403.
(72) Wu, W. K.; Cho, C. H.; Lee, C. W.; Wu, K; Fan, D; Yu, J; Sung, J. J. Proteasome inhibition: a new therapeutic strategy to cancer treatment. *Cancer Lett.* **2010**, *293*, 15–22.
(73) Richardson, P. G.; Barlogie, B.; Berenson, J.; Singhal, S.; Jagannath, S.; Irwin, D.; Rajkumar, S. V.; Srkalovic, G.; Alsina, M.; Alexanian, R.; Siegel, D.; Orlowski, R. Z.; Kuter, D.; Limentani, S. A.; Lee, S.; Hideshima, T.; Esseltine, D.-L.; Kauffman, M.; Adams, J.; Schenkein, D. P.; Anderson, K. C. A phase 2 study of bortezomib in relapsed, refractory myeloma. *New Engl. J. Med.* **2003**, *348*, 2609–2617.
(74) Richardson, P. G.; Briemberg, H.; Jagannath, S.; Wen, P. Y.; Barlogie, B.; Berenson, J.; Singhal, S.; Siegel, D. S.; Irwin, D.; Schuster, M.; Srkalovic, G.; Alexanian, R.; Rajkumar, S. V.; Limentani, S.; Alsina, M.; Orlowski, R. Z.; Najarian, K.; Esseltine, D.; Anderson, K. C.; Amato, A. A. Frequency, characteristics, and reversibility of peripheral neuropathy during treatment of advanced multiple myeloma with bortezomib. *J. Clin. Oncol.* **2006**, *24*, 3113–3120.
(75) Lonial, S.; Waller, E. K.; Richardson, P. G.; Jagannath, S.; Orlowski, R. Z.; Giver, C. R.; Jaye, D. L.; Francis, D.; Giusti, S.; Torre, C.; Barlogie, B.; Berenson, J. R.; Sunghal, S.; Schenkein, D. P.; Esseltine, D. L. W.; Anderson, J.; Xiao, H.; Heffner, L. T.; Anderson, K. C. Risk factors and kinetics of thrombocytopenia associated with bortezomib for relapsed, refractory multiple myeloma. *Blood* **2005**, *106*, 3777–3784.
(76) Blanquicett, C.; Roman, J.; Hart, C. M. Thiazolidinediones as anti-cancer agents. *Cancer Ther.* **2008**, *6*, 25–34.
(77) He, B. C.; Chen, L.; Zuo, G. W.; Zhang, W.; Bi, Y.; Huang, J.; Wang, Y.; Jiang, W.; Luo, Q.; Shi, Q.; Zhang, B. Q.; Liu, B.; Lei, X.; Luo, J.; Luo, X.; Wagner, E. R.; Kim, S. H.; He, C. J.; Hu, Y.; Shen, J.; Zhou, Q.; Rastegar, F.; Deng, Z. L.; Luu, H. H.; He, T. C.; Haydon, R. C. Synergistic antitumor effect of the activated PPARgamma and retinoid recptors on human osteosarcoma. *Clin. Cancer Res.* **2010**, *16*, 2235–2245.
(78) Lee, J. Y.; Kim, J. K.; Cho, M. C.; Shin, S.; Yoon, D. Y.; Heo, Y. S.; Kim, Y. Cytotoxic flavonoids as agonists of peroxysome proliferator-activated receptor gamma on human cervical and prostate cancer cells. *J. Nat. Prod.* **2010**, *73*, 1261–1265.
(79) Reka, A. K.; Kurapati, H.; Narala, V. R.; Bommer, G.; Chen, J.; Standiford, T. J.; Keshamouni, V. G. Peroxisome proliferator-activated receptor-gamma activation inhibits tumor metastasis by antagonizing Smad3-mediated epithelial-mesenchymal transition. *Mol. Cancer Res.* **2010**, *9*, 3221–3232.

(80) Voutsadakis, I. A. Peroxisome proliferator activated receptor-gamma and the ubiquitin-proteasome system in colorectal cancer. *World J. Gastrointest. Oncol.* **2010**, *2*, 235–241.

(81) Knight, Z. A.; Lin, H.; Shokat, K. M. Targeting the cancer kinome through polypharmacology. *Nat. Rev. Cancer* **2010**, *10*, 130–137.

(82) Fedorov, O.; Müller, S.; Knapp, S. The (un)target cancer kinome. *Nat. Chem. Biol.* **2010**, *6*, 166–169.

(83) Gossage, L.; Eisen, T. Targeting multiple kinase pathways: a change in paradigm. *Clin. Cancer Res.* **2010**, *16*, 1973–1978.

(84) Agrawal, P. K.; Jain, D. C. ^{13}C NMR spectroscopy of oleanane triterpenoids. *Prog. NMR Spectrosc.* **1992**, *24*, 1–90.

(85) Mahato, S. B.; Kundu, A. P. ^{13}C NMR spectra of pentacyclic triterpenoids — a compilation and some salient features. *Phytochemistry* **1994**, *37* (6), 1517–1575.

(86) Friesner, R. A.; Murphy, R. B.; Repasky, M. P.; Frye, L. L.; Greenwood, J. R.; Halgren, T. A.; Sanschagrin, P. C.; Mainz, D. T. Extra precision Glide: Docking and scoring incorporating a model of hydrophobic enclosure for protein-ligand complexes. *J. Med. Chem.* **2006**, *49*, 6177–6196.

(87) Arrigo, A. P.; Tanaka, K.; Goldberg, A. L.; Welch, W. J. Identity of the 19S 'prosome' particle with the large multifunctional protease complex of mammalian cells (the proteasome). *Nature (London)* **1988**, *331*, 192–194.

(88) Sadowski, J. A hybrid approach for addressing ring flexibility in 3D database searching. *J. Comput.-Aided Mol. Des.* **1997**, *11*, 53–60.

(89) Moravec, R. A.; O'Brien, M. A.; Daily, W. J.; Scurria, M. A.; Bernad, L.; Riss, T. L. Cell-based bioluminescent assays for all three proteasome activities in a homogeneous format. *Anal. Biochem.* **2009**, *387*, 294–302.

(90) Lamoral-Theys, D.; Pottier, L.; Kerff, F.; Dufrasne, F.; Proutière, F.; Wauthoz, N.; Neven, P.; Ingrassia, L.; Van Antwerpen, P.; Lefranc, F.; Gelbcke, M.; Pirotte, B.; Kraus, J. L.; Nève, J.; Kornienko, A.; Kiss, R.; Dubois, J. Simple di- and trivanillates exhibit cytostatic properties toward cancer cells resistant to pro-apoptotic stimuli. *Bioorg. Med. Chem.* **2010**, *18*, 3823–3833.